The Use of Micro-jets for Airfoil Self-noise Control

Máté Szőke[*], Daniele Fiscaletti[†] and Mahdi Azarpeyvand[‡]

University of Bristol, Bristol, BS8 1TR, United Kingdom

The current work is an experimental investigation on the use of open-loop flow control techniques to reduce trailing edge noise of a flat plate. An array of inclined transverse jet nozzles is placed upstream of the trailing edge, with the aim of controlling the hydrodynamic pressure field associated with the boundary layer. The turbulence statistics downstream of the flow control section were measured with the use of hot-wire anemometry, while the simultaneous measurement of the surface pressure fluctuations was performed with flush mounted microphones. It is shown that the proposed flow control method leads to a reduction of the energy content of the surface pressure fluctuations in the region of low and mid frequencies. The spanwise correlation length of the turbulent structures near the trailing edge is also observed to decrease as a consequence of using multiple jet injections. In general, results have shown that the proposed flow control technique can alter the boundary layer structure, and it has the potentials to reduce far-field trailing edge noise.

I. Introduction

Noise generated by the turbulence around an airfoil has potentials to give a significant contribution to environmental noise pollution, as airfoils are used in a vast number of engineering applications. The broadband noise generated by an airfoil in movement inside of a fluid mainly originates from the turbulent boundary layer trailing edge (TE) noise [1]. The reduction of trailing edge noise is therefore an important engineering challenge. The problem has been of interest since the 1970s, when the first pioneering studies were conducted to understand the mechanism leading to trailing edge noise [2–8]. A broadband far-field noise is produced as the hydrodynamic pressure field associated to the boundary layer reaches the trailing edge, where it scatters into sound.

Two general strategies exist to attenuate the trailing edge noise. In particular, changes introduced to the geometry of the trailing edge (i.e. the scattering condition) can be classified as *passive* noise reduction methods. Examples of the passive methods are the TE serrations [9–16], TE brushes [17,18], porous materials [19–24], surface treatments [25–28], shape optimization and morphing [29]. The main advantages of the passive methods are their geometrical simplicity, and their low manufacturing and maintenance costs. On the other hand, their performance in terms of noise attenuation is tailored to a given range of conditions, and outside this range these methods could introduce an undesired decrease in aerodynamic performance, or an increase in noise emission. The other possibility to attenuate trailing edge noise is to control the pressure field associated to the boundary layer upstream of the trailing edge with the use of flow control techniques, which can be classified as *active* noise control methods. The present research focuses on the use of transverse jets to mitigate the trailing edge noise, which belongs to the family of the active flow control techniques. The jet injection is applied in a configuration of open-loop control, where the speed of the jet injection is varied independently of the emitted far-field noise or the freestream flow speed. With the aim of enhancing the performances of flow control, the present work tries to understand how jet injection can attenuate trailing edge noise.

Trailing edge noise models [1, 7, 30, 31] reveal the physical quantities that are mainly responsible for the generation of trailing edge noise. The currently examined flow control method is aimed at targeting these flow properties to achieve noise attenuation. The noise model developed by Amiet [7] is introduced in Section II C

[*]PhD Student, Faculty of Engineering, University of Bristol, Bristol, United Kingdom, BS8 1TR
[†]Lecturer, Faculty of Engineering, University of Bristol, Bristol, United Kingdom, BS8 1TR
[‡]Reader, Faculty of Engineering, University of Bristol, Bristol, United Kingdom, BS8 1TR

of this paper, and it is considered in the current study to establish the link between the turbulence and far-field noise generation. The model reveals that the spectra of the surface pressure fluctuations (ϕ_{pp}) and the spanwise extent of the turbulent structures (Λ_z) are the dominant components responsible for the generation of trailing edge noise. Favourable changes on these quantities can, therefore, result in the reduction of far-field noise.

Injection into or suction from the boundary layer result in a reduction of the spectral content of the surface pressure fluctuations, and of the spanwise extent of the turbulent structures. These techniques can overcome the drawbacks of the passive methods, and enhance the performances in terms of achievable noise reduction. Moreover, controllability is a significant advantage of the active methods, while their main disadvantage is their need of an external power. The power intake of any flow control techniques must be kept low. Szőke and Azarpeyvand [32] showed that the hydrodynamic pressure field associated with the boundary layer can be efficiently modified by the use of active flow control techniques. Their study focused on the application of uniform steady perpendicular and inclined blowing. The authors showed that by inclining the direction of the flow control, the energy requirement reduces without affecting the levels of noise attenuation. As a continuation of their work, the current paper aims to investigate the use of inclined transverse micro-jets in place of a uniform blowing, and examine further reduction of the intake energy by such flow control technique.

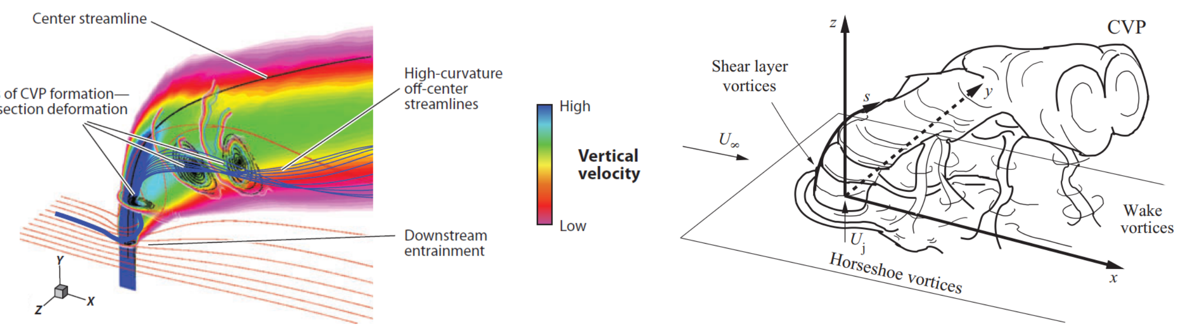

(a) CFD results at $r = 5.7$ (Muppidi & Mahesh [33])

(b) Flow structure model at $2 < r < 10$ (Fric and Roshko [34])

Figure 1. The flow structure downstream of a transverse jet in incompressible flow

The problem of transverse jets, or jets in a cross-flow, was extensively studied in the past [33–35]. The resulting flow structure was observed to be dependent on the velocity ratio (r), i.e the ratio of jet velocity to the mean cross flow velocity ($r = u_{jet}/u_\infty$). At $r < 2$, the jet remains close to the wall, and only a counter-rotating vortex pair can be identified downstream. At $r > 2$, the jet is able to penetrate the free-stream flow, and the flow pattern becomes more complex (see Fig. 1). Among the vast number of engineering applications where transverse jets were proven to be effective, the cooling of gas turbine blades is the most relevant to the current work. When using jets for cooling purposes, jets fluid should flow on the wall in order to increase heat dissipation. Similarly, a flow pattern where a stable and low energy fluid is formed over the wall of the airfoil can result in noise attenuation. Therefore, the geometries considered in the studies on gas turbine blade cooling can give a good basis to define the properties of the inclined traverse jets for trailing edge noise attenuation purposes. In these works [36–42], the jets were circular in shape (diameter D), inclined 30° with respect to the wall and spaced $3.5D$ apart from each other. Additionally, the velocity ratio was kept below $r = 2$. The circular shape, the shallow inclination and the spacing of the jet nozzles are similar to those proposed for gas turbine blade cooling. However, the flow associated with the generation of the trailing edge noise has significantly higher turbulence levels than the flow around gas turbine blades, therefore the two applications lead to different flow structures. The ratio of jet diameter to the thickness of the boundary layer is less then unity in the current work, therefore, the currently applied jets can be considered as "micro-jets". As a main goal of the present work, it is important to examine the effect of transverse jets on ϕ_{pp} and Λ_z in order to draw conclusions over the aeroacoustic efficiency of the present flow control technique. Previous studies focusing on transverse jets, however, failed to provide these information, which results in a gap in the literature. The aim of the current experimental work is to fill this gap by investigating the effect of transverse jets on turbulence statistics and surface pressure fluctuations. Estimating these parameters could help us understand how the jets affect the boundary layer and the turbulence in the near-wall region.

The current paper is organised as follows. Section II describes the measurement conditions, the experimental set-up, the geometrical properties relevant to the experimental investigation, and introduces Amiet's trailing edge noise model, which establishes the link between the flow properties and the emitted far-field noise. Section III discusses the resulting flow structure. Once the hydrodynamic flow structure is understood, its effects on the trailing edge noise generation are evaluated.

II. Experimental Approach

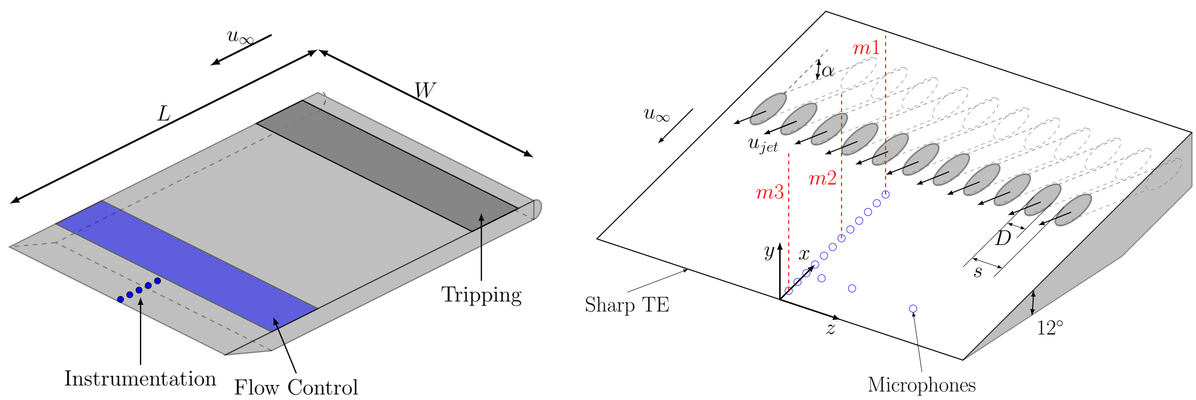

(a) Overall view of the rig (b) Detailed view of the instrumented and active flow control area

Figure 2. Schematic view of the rig and the trailing edge

A. Test Rig Set-up and Instrumentation

Experiments were conducted in the open jet closed-circuit wind tunnel facility, at the University of Bristol. A long (L =1 m), zero pressure gradient flat plate ending in a sharp (12°) trailing edge was built as schematically shown in Fig. 2(a). Tests have been carried out at a uniform flow velocity of $u_\infty = 15$ m/s, corresponding to a Reynolds number of 10^6, based on the length of the plate ($Re = u_\infty L/\nu$). The turbulence intensity of the flow in the test section is approximately 2 %. The boundary layer transition was triggered by means of installing an 80-grit sandpaper aft the elliptical leading edge of the plate. The coordinate system is defined in Fig. 2.

Flush mounted FG-23329-P07 type Knowles electret condenser microphones were used for the measurement of the boundary layer unsteady surface pressure fluctuations. A total number of 21 transducers were distributed both in the streamwise and spanwise directions close to the trailing edge, as shown in Fig. 2(b). The miniature microphones were calibrated prior to the measurements, and their uncertainty was found to be ±0.5 dB within the investigated frequency range assuming a normal distribution of pressure fluctuations [43]. The microphones were mounted below a pinhole with a diameter of $d = 0.4$ mm. The attenuation of the pressure signal can be considered negligible, should the dimensionless pinhole diameter ($d^+ = du_\tau/\nu$) be below $d^+ = 19$ (see Schewe [44]). The current configuration resulted in $d^+ \approx 17$, therefore the pressure attenuation introduced by the pinhole is negligible. In addition, the discontinuity on the surface does not have any significant influence on the boundary layer. The corrections proposed by Corcos [45] were applied during the post processing of the microphone signals. Measurements were taken at three different microphone locations along the centreline ($z = 0$), referred to as $m1$, $m2$ and $m3$, corresponding to x/L = -9.9, -6.5, -0.45 %, respectively.

Dantec 55P16 type single-sensor hot-wire probes were used to measure the turbulence statistics of the flow velocity over the entire boundary layer (along the y axis) at axial locations $m1$, $m2$ and $m3$. The probes were operated by a Dantec StreamWare Pro CTA91C10 module, at an overheat ratio of 1.8. Their uncertainty was found to be less than 0.5 % over the entire range of investigated velocities. The data was acquired simultaneously from the microphones and the hot-wire using a National Instruments PXIe-4499 system, at a sampling rate of f_s =65,536 Hz (= 2^{16} Hz), for a time period of 16 seconds. Data processing was performed with the use of Python's SciPy package. When calculating spectra and coherence, a filter was applied in order to reduce low frequency measurement noise [46]. Time signals were divided into smaller segments with a 50 % overlapping. The length of the time segments (WS) was defined such that the frequency resolution ($\Delta f = 4f_s/WS$) of the transformed signal was $\Delta f = 64$ Hz. Hamming windowing was then applied on each segment, which was followed by the calculation of their fast Fourier transform (FFT). After the Fourier transform of each segment, the energy loss in the signal caused by the application of Hamming windowing was compensated, and the FFT results were averaged to achieve a smooth resolution of spectra in the frequency domain.

B. Parameters of the Active Flow Control Method

A line distribution of micro-jets was placed on the test rig at $x/L = -0.12$, as shown in Fig. 2(b). The diameter ($D = 4$ mm), the nozzle length-to-diameter ratio ($l/D = 5$), and the spacing ($s = 10$ mm) of the jets were kept constant, while the jet inclination angle (α) was set at three different angles: $\alpha = 15°$, $30°$ and $45°$.

The flow control severity (σ) is defined after Antonia *et al.* [47]. This parameter relates the momentum of the applied blowing to the momentum deficit of the boundary layer. Considering the properties of the current problem, the flow control severity can be expressed as

$$\sigma = \frac{u_{jet} A_{noz}/s}{\theta_0 u_\infty}, \tag{1}$$

where u_{jet} is the magnitude of the jet velocity, A_{noz} is the cross section area of a single jet nozzle, $u_\infty = 15$ m/s is the freestream flow velocity, $s = 2.5D$ is the spacing of the jets, and θ_0 is the momentum thickness of the baseline boundary layer ($r = 0$). Additional flow properties significant to the problem under analysis are the jet Reynolds number Re_{jet}, velocity ratio $r = u_{jet}/u_\infty$, and momentum flux ratio $J = \varrho_{jet} u_{jet}^2 / \varrho u_\infty^2$. The values of σ adopted in the experiments, and the associated properties of the jets and the boundary layer are presented in Table 1.

Table 1. Boundary layer and flow control properties measured at location $m3$

u_∞ [m/s]	σ [–]	δ [mm]	δ^* [mm]	θ [mm]	Re_{jet} [–]	Re_θ [–]	r [–]
15	0	31.0	5.45	3.90	0	3900	0
15	0.4	31.4	5.30	3.92	5300	3920	1.33
15	0.6	31.6	5.02	3.98	7200	3980	1.80

C. Amiet's Trailing Edge Noise Model

The important quantities driving the TE noise generation can be readily found from the TE noise models [1, 7, 30]. One of the most widely used analytical models is that of Amiet [7]. The model links the turbulent statistics of the boundary layer to the far-field pressure power spectra (S_{pp}), by assuming frozen turbulence over the wall. Amiet defined the far-field noise as

$$S_{pp}(x, y, z = 0, f) = \left(\frac{fLy}{4\pi c_0 \xi^2}\right)^2 \frac{W}{2} |\mathcal{L}|^2 \Lambda_z(f) \phi_{pp}(f, x = y = z = 0), \tag{2}$$

where f denotes frequency, c_0 is the speed of sound, $\xi = x^2 + (1 - u_\infty/c_0)^2 y^2$, L is the length of the plate (chord), W is the width of the plate, $\mathcal{L}$ is the gust response transfer function, Λ_z is the spanwise length of turbulent structures within the boundary layer, and ϕ_{pp} is the power spectra of surface pressure fluctuations. For a more detailed description and for the derivation of the model, we refer to Amiet [5, 7]. Eq. (2) reveals that the trailing edge noise is mainly driven by the product between the power spectra of the surface pressure fluctuations (ϕ_{pp}), and the spanwise extent of turbulent structures (Λ_z). The trubulent structures associated with the turbulent boundary layer exert pressure fluctuations on the surface. A reduction of the turbulent energy is therefore required to reduce the power spectra of the surface pressure fluctuations.

While ϕ_{pp} is measured directly using flush-mounted pressure transducers, Λ_z is calculated using

$$\Lambda_z(f) = \sum_{i=1}^{n} \sqrt{\gamma_z^2(\Delta z_i)} \Delta z_i, \tag{3}$$

where γ_z^2 is the normalized cross-spectra between the signals collected from the transducers distributed over the span of the plate near the trailing edge ($x/L = -1.46$ %), Δz is the separation distance between the microphones, and n is the number of separation distances, i.e. microphone pairs. The geometry constraints associated with the finite size of the microphones make it difficult to estimate γ_z^2 for small separation distances (Δz). However, Eq. (3) reveals that the changes observed in γ_z^2 can be directly related to the changes of the spanwise length of the turbulent structures. To this purpose, three microphone spacings were considered in the current work to assess the effect of flow control on the size of the turbulent structures, where Δz = 3.6 mm, 7.8 mm and 11.4 mm. The main goal of the present work is therefore to measure ϕ_{pp} and Λ_z, and to evaluate the effect of the proposed flow control method on them. Additional turbulence quantities such as Reynolds shear stresses, frequency-energy content within the boundary layer, temporal cross and auto-correlation can also be used to gain an insight into the noise generation mechanism. The effects of the present flow control technique on these quantities are discussed in the following section.

III. Results

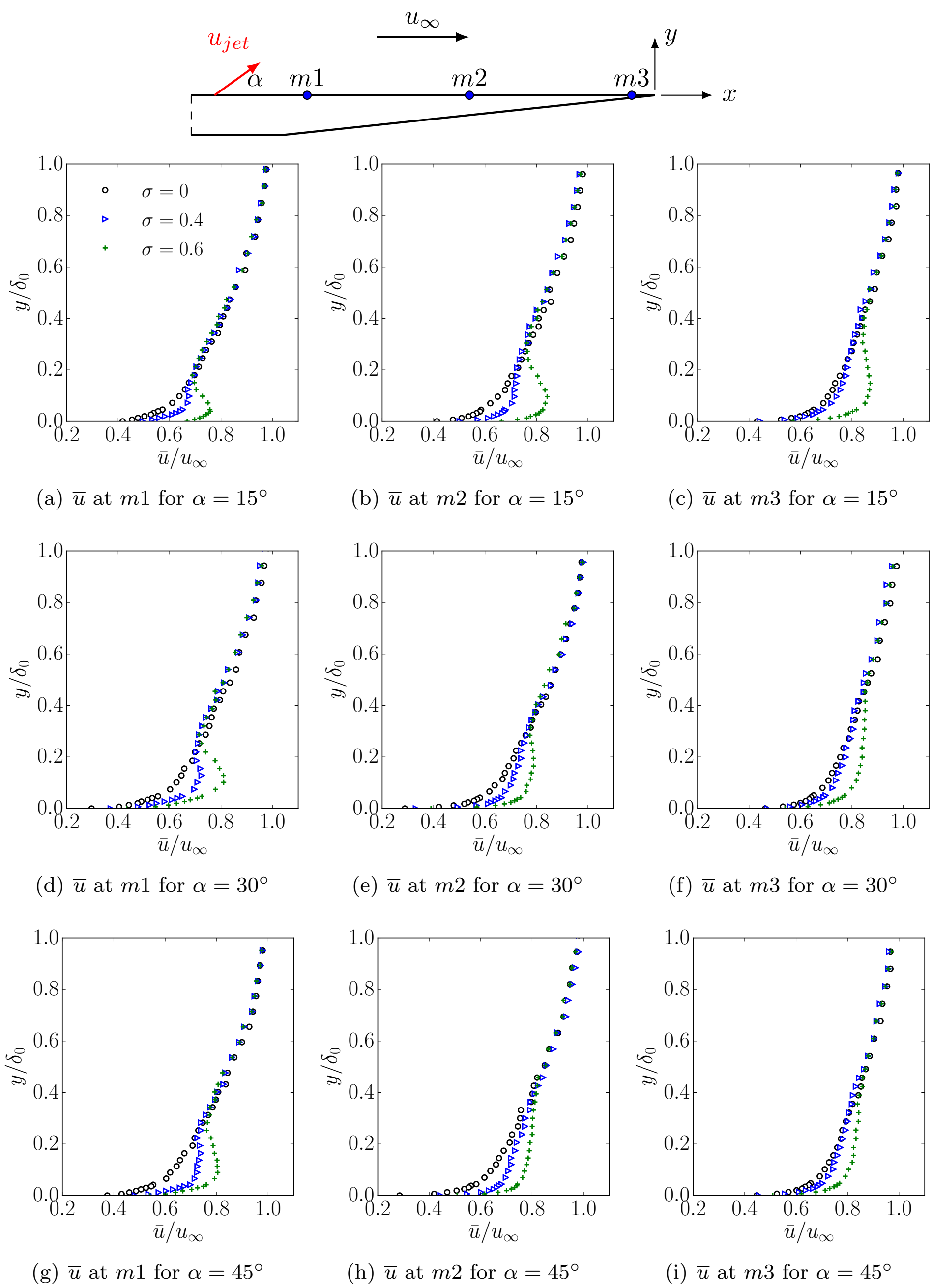

(a) $\overline{u}$ at $m1$ for $\alpha = 15°$ (b) $\overline{u}$ at $m2$ for $\alpha = 15°$ (c) $\overline{u}$ at $m3$ for $\alpha = 15°$

(d) $\overline{u}$ at $m1$ for $\alpha = 30°$ (e) $\overline{u}$ at $m2$ for $\alpha = 30°$ (f) $\overline{u}$ at $m3$ for $\alpha = 30°$

(g) $\overline{u}$ at $m1$ for $\alpha = 45°$ (h) $\overline{u}$ at $m2$ for $\alpha = 45°$ (i) $\overline{u}$ at $m3$ for $\alpha = 45°$

Figure 3. Mean velocity profiles at locations $m1, m2$ and $m3$ for $\alpha = 15°$, $30°$ and $45°$

Figure 3 presents the mean velocity ($\bar{u}$) measured over the entire boundary layer at axial locations $m1$, $m2$ and $m3$ for three jet inclination angles ($\alpha = 15°$, $30°$ and $45°$) and three blowing rates ($\sigma = 0, 0.4$ and 0.6). The results reveal that the jets increase the momentum close to the wall. Downstream of $m1$, the increase in $\bar{u}$ spreads wider in the y-direction, which indicates that the jets keep penetrating into the boundary layer at increasing downstream locations. However, the effect of the jets are confined to the near-wall region, as peak in $\bar{u}$ is observed in the range of $0.1 - 0.2\delta_0$ at all locations. The upper half of the boundary layer is unaffected by the jets. The results suggest that the jet inclination angle does not have a significant effect on the $\bar{u}$ results. However, as α increases the jets penetrate at higher wall-normal locations within the boundary layer. Also, the observed mean velocity profiles indicate no sign of separation regardless of the applied blowing rate or jet inclination angle. The lack of separation is associated with a lower amount of drag compared to the uniform blowing [32], where separation is observed to occur. The observed increase in $\bar{u}$ leads to drag reduction, given that the momentum deficit in the boundary layer is directly proportional to the drag produced by the viscous forces.

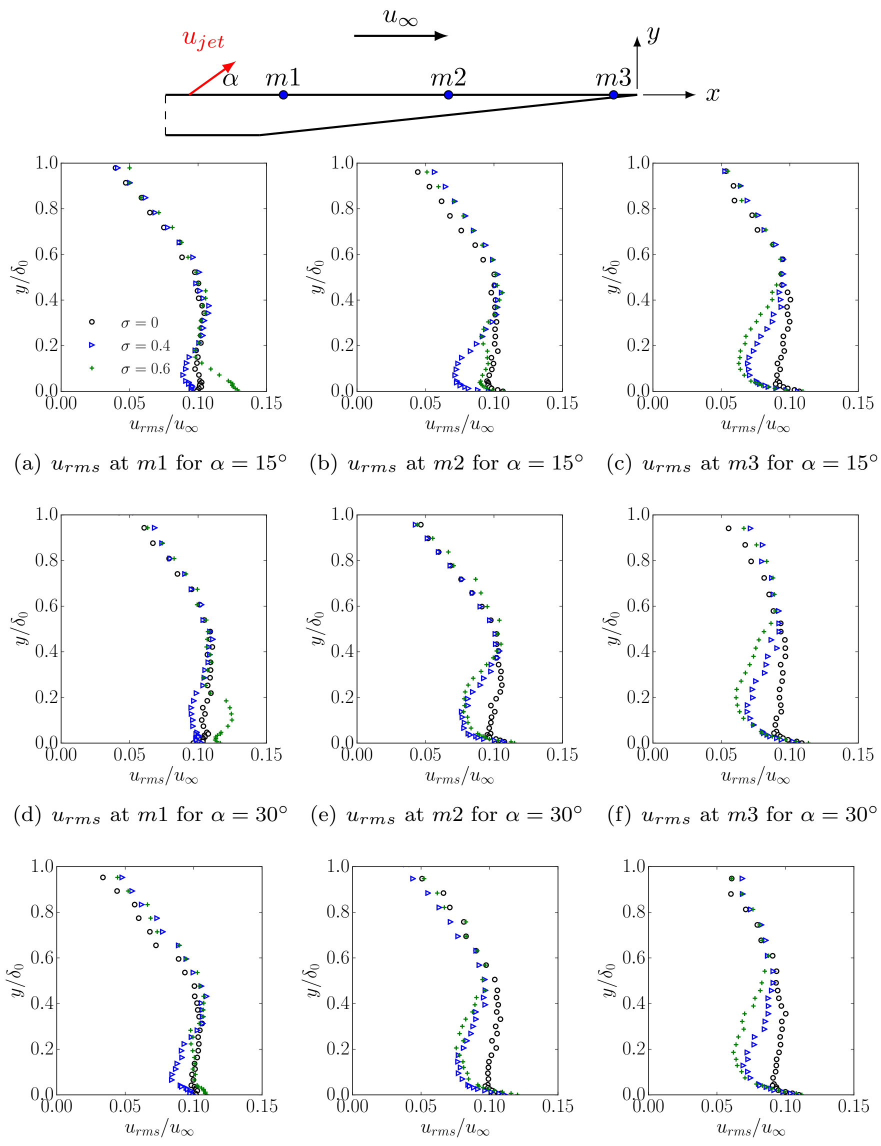

(a) u_{rms} at $m1$ for $\alpha = 15°$ (b) u_{rms} at $m2$ for $\alpha = 15°$ (c) u_{rms} at $m3$ for $\alpha = 15°$

(d) u_{rms} at $m1$ for $\alpha = 30°$ (e) u_{rms} at $m2$ for $\alpha = 30°$ (f) u_{rms} at $m3$ for $\alpha = 30°$

(g) u_{rms} at $m1$ for $\alpha = 45°$ (h) u_{rms} at $m2$ for $\alpha = 45°$ (i) u_{rms} at $m3$ for $\alpha = 45°$

Figure 4. Root mean square velocity velocity profiles at locations $m1, m2$ and $m3$ for $\alpha = 15°$, $30°$ and $45°$

The root mean square (rms) of the flow velocity is presented in Fig. 4, for the axial locations $m1$, $m2$ and $m3$, for the three considered jet inclination angles ($\alpha = 15°$, $30°$ and $45°$), and at the three considered blowing rates ($\sigma = 0, 0.4$ and 0.6). The use of inclined transverse jets reduced the energy content within the boundary layer. At $m1$, an increase of u_{rms} is observed for $\sigma = 0.6$ in the near-wall region for all inclination angles, but for the lower blowing rate ($\sigma = 0.4$), a reduction of u_{rms} takes place at $m1$. At $m2$ and $m3$, a decrease in u_{rms} evidence a lower energy content for all σ and α cases. The largest amount of reduction in u_{rms} is achieved at the core of the jets, i.e. in the region $0.1 - 0.2\delta_0$. The blowing exerts its effect downstream of the jet nozzles, which is confirmed by the reduction of u_{rms} along the streamwise direction. A possible explanation for these observations is that the flow within the jets is laminar, and therefore it is characterised by a lower energy content than the turbulent boundary layer. The observed energy attenuation can lead to a reduction of surface pressure fluctuations, which is the basis of noise attenuation at the trailing edge.

Higher values of σ result in a stronger reduction of u_{rms}, but it could also induce flow separation, therefore additional experiments are planned to find the optimal blowing rate.

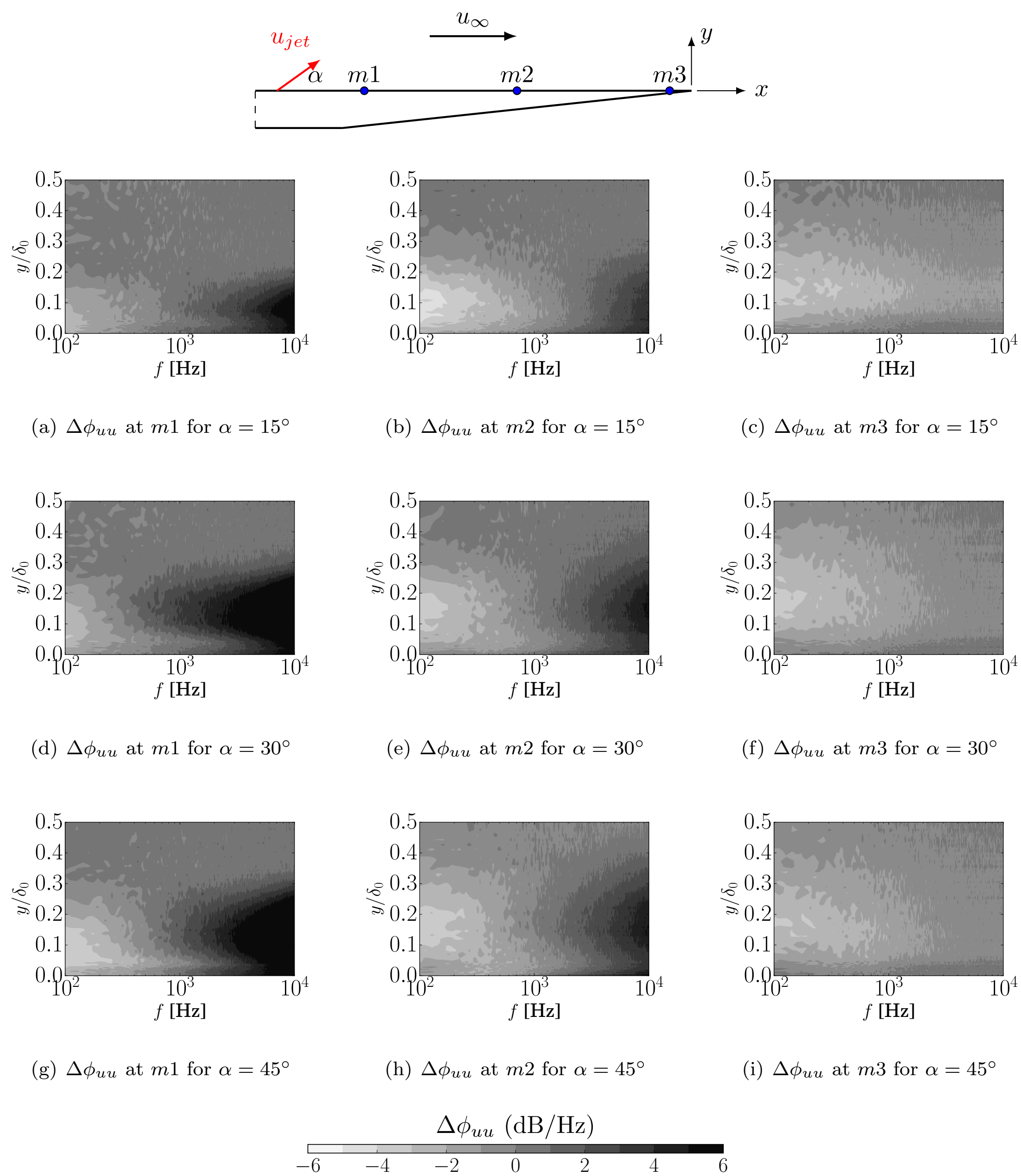

(a) $\Delta\phi_{uu}$ at $m1$ for $\alpha = 15°$

(b) $\Delta\phi_{uu}$ at $m2$ for $\alpha = 15°$

(c) $\Delta\phi_{uu}$ at $m3$ for $\alpha = 15°$

(d) $\Delta\phi_{uu}$ at $m1$ for $\alpha = 30°$

(e) $\Delta\phi_{uu}$ at $m2$ for $\alpha = 30°$

(f) $\Delta\phi_{uu}$ at $m3$ for $\alpha = 30°$

(g) $\Delta\phi_{uu}$ at $m1$ for $\alpha = 45°$

(h) $\Delta\phi_{uu}$ at $m2$ for $\alpha = 45°$

(i) $\Delta\phi_{uu}$ at $m3$ for $\alpha = 45°$

Figure 5. Changes in the velocity power spectral density for $\sigma = 0.4$ with respect to the baseline case ($\sigma = 0$) at $m1, m2$ and $m3$ for $\alpha = 15°$, $30°$ and $45°$

The power spectral density (PSD) of the flow velocity enables us to assess at which frequencies the u_{rms} attenuation occurs. The size of the turbulent structures is inversely proportional to the frequency of their footprint, which was measured by the flush mounted microphones, therefore the PSD results also provide a description of how the jets affect the streamwise extent of the turbulent structures. The change of the power spectral density in consequence of the flow control technique is defined as $\Delta\phi_{uu} = \phi_{uu,treated} - \phi_{uu,baseline}$ (dB/Hz). Results are presented in Fig. 5 for the lower blowing rate ($\sigma = 0.4$). At $m1$, for all cases of α, the jets result in a reduction of ϕ_{uu} at low frequencies (below 1 kHz), while a significant increase of the spectral content is observed at high frequencies (above 1 kHz). These observations suggest that the turbulent kinetic energy has a larger probability to be contained within smaller scales of turbulence in consequence of multiple jets injection. It is anticipated that these smaller turbulent structures are generated by the interaction between the jets and the wall, resulting in an increase of the shear in this area. However, downstream of $m1$, the spectral increase observed at higher frequencies disappears for all angles under analysis, while the reduction in ϕ_{uu} strengthens at low frequencies. In proximity to the trailing edge ($m3$), $\Delta\phi_{uu}$ indicates a reduction at all frequencies. As the fluid of the jets enters the boundary layer, it locally reduces the energy content within the flow, which leads to the observed reduction in the spectral content at low frequencies.

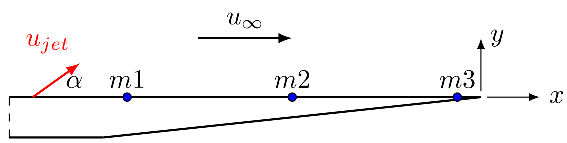

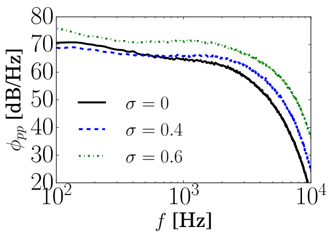

(a) $\phi_{pp}(f)$ at $m1$, $\alpha = 15°$

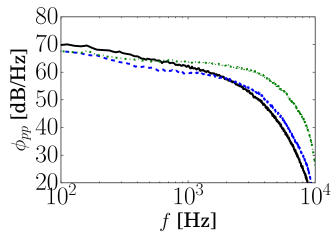

(b) $\phi_{pp}(f)$ at $m2$, $\alpha = 15°$

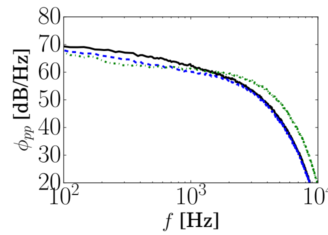

(c) $\phi_{pp}(f)$ at $m3$, $\alpha = 15°$

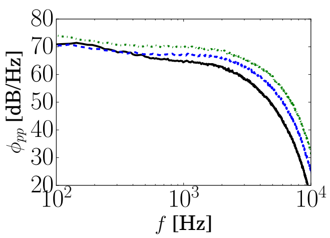

(d) $\phi_{pp}(f)$ at $m1$, $\alpha = 30°$

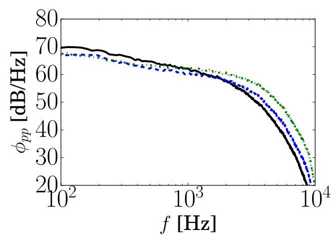

(e) $\phi_{pp}(f)$ at $m2$, $\alpha = 30°$

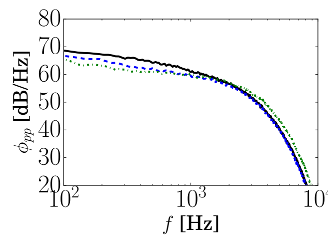

(f) $\phi_{pp}(f)$ at $m3$, $\alpha = 30°$

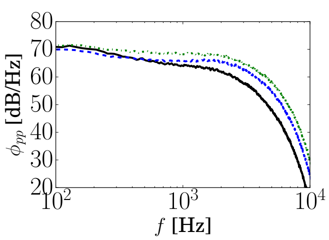

(g) $\phi_{pp}(f)$ at $m1$, $\alpha = 45°$

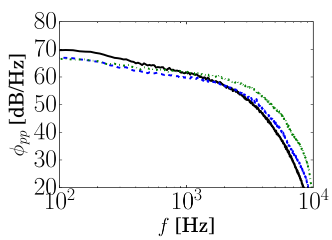

(h) $\phi_{pp}(f)$ at $m2$, $\alpha = 45°$

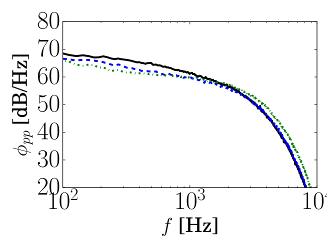

(i) $\phi_{pp}(f)$ at $m3$, $\alpha = 45°$

Figure 6. Surface pressure spectra at $m1$, $m2$ and $m3$ for $\alpha = 15°$, $30°$ and $45°$

According to Amiet's model [7], the power spectral density of the surface pressure fluctuations (ϕ_{pp}) is one of the dominant quantities driving the generation of trailing edge noise. The surface pressure PSD was calculated for $m1$, $m2$ and $m3$, for the three α and three σ cases. The results are presented in Fig. 6. The jet inclination angle (α) has been observed to have a negligible effect on the surface pressure fluctuations. At $m1$, an increase is observed in the spectral energy content independent of α and σ, which is consistent with the results presented in Figs. 4 and 5. At $m2$ and $m3$, a significant reduction in the spectral content is observed at low frequencies for both cases of $\sigma > 0$, which becomes more significant at lower frequencies, as the flow reaches the trailing edge ($m3$). At the trailing edge ($m3$), a slight increase of ϕ_{pp} is observed for $\sigma = 0.6$, for frequencies above 2 kHz. Nonetheless, the reduction gained at low frequencies (below 2 kHz) is stronger at the higher blowing rate ($\sigma = 0.6$) than at the lower blowing rate ($\sigma = 0.4$). A reduction at low frequency component of the far-field noise is of particular interest for engineering applications, as the low frequency aerodynamically generated noise can propagate over longer distances than the high frequency noise. In order to understand the overall effect of the jets on the trailing edge noise, the spanwise extent of turbulent structures also need to be investigated.

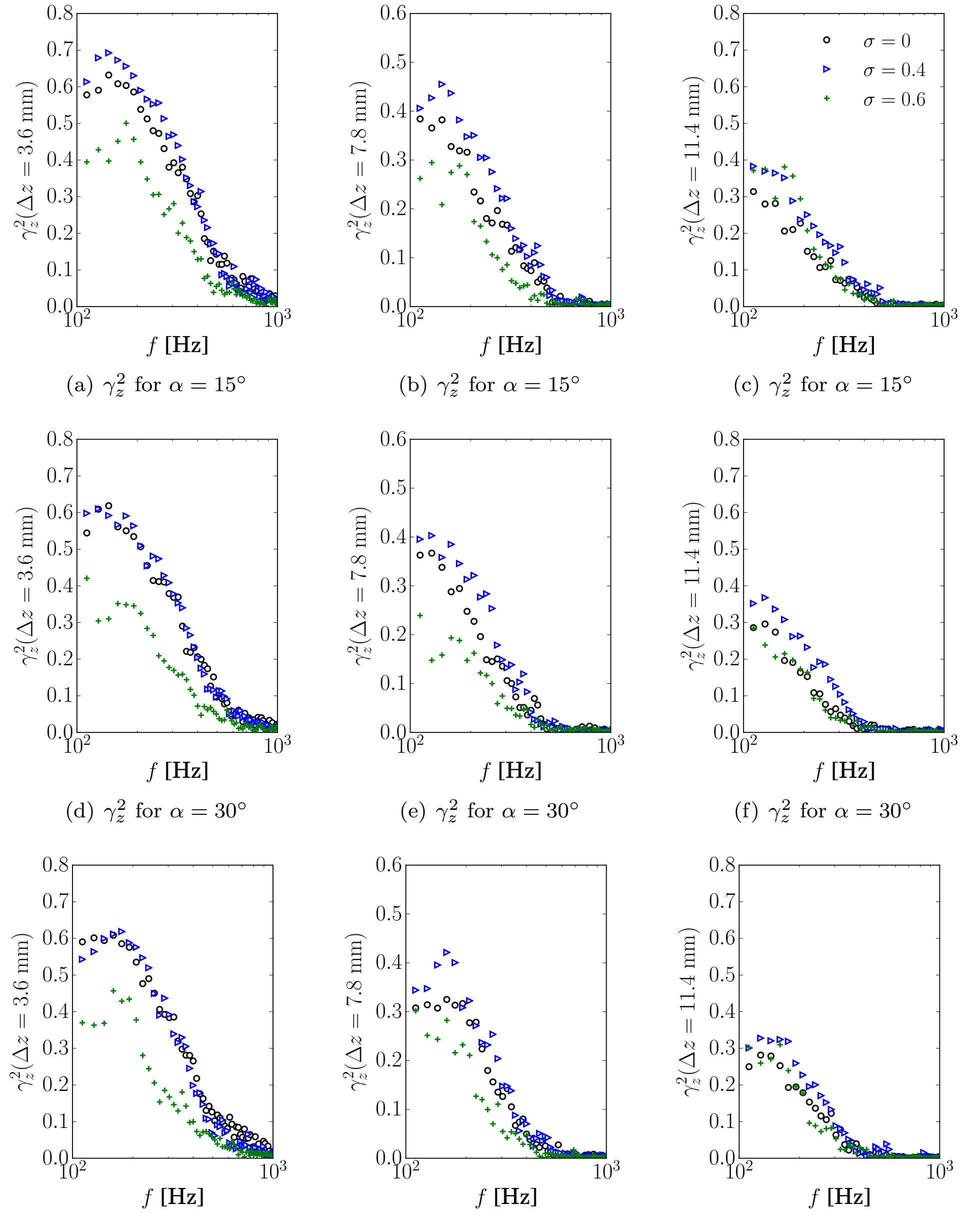

(a) γ_z^2 for $\alpha = 15°$ (b) γ_z^2 for $\alpha = 15°$ (c) γ_z^2 for $\alpha = 15°$

(d) γ_z^2 for $\alpha = 30°$ (e) γ_z^2 for $\alpha = 30°$ (f) γ_z^2 for $\alpha = 30°$

(g) γ_z^2 for $\alpha = 45°$ (h) γ_z^2 for $\alpha = 45°$ (i) γ_z^2 for $\alpha = 45°$

Figure 7. Spanwise coherence at $x/L = -1.46$ % for $\alpha = 15°$, $30°$ and $45°$

The spanwise coherence (γ_z^2), describing the spanwise extent of the turbulent structures at the trailing edge is presented in Fig. 7, for $\alpha = 15°, 30°$, and $45°$, and for $\sigma = 0, 0.4$ and 0.6. It is observed that different jet inclination angles result in very similar values of coherence. The lower blowing rate ($\sigma = 0.4$) results in a slight increase of spanwise coherence at all the different microphone spacings under analysis. This increase is more pronounced at larger separation distances (Δz =7.8 mm and 11.4 mm), i.e. for larger structures.

The larger blowing rate ($\sigma = 0.6$) results in the reduction of the spanwise coherence for $\Delta z = 3.6$ mm and 7.8 mm, while γ_z^2 is comparable to the baseline case for $\Delta z = 11.4$ mm.

As discussed in Section II, the generation of trailing edge noise is driven by the product between ϕ_{pp} and Λ_z [7], therefore the reduction achieved in the product of these two terms can result in the reduction of far-field noise. It has been understood from the results presented in the current work that the amplitudes of the pressure fluctuations at the trailing edge are attenuated at the low and mid frequencies by multiple jets injection, when the lower blowing rate was applied. Considering the higher blowing rate, it was found that a significant attenuation of ϕ_{pp} is achieved at low frequencies, with a modest penalty paid at high frequencies. The other term in the product of the far-field noise model, Λ_z, was estimated through the spanwise coherence at three different Δz. It is understood from the results of spanwise coherence that the lower blowing rate increased the spatial extent of the turbulent structures. The application of higher blowing rate, however, reduces the size of the turbulent structures. Considering Amiet's noise model, it can be concluded that the multiple jets applied with a lower blowing rate are capable of reducing the far-field noise at low frequencies. With respect to the higher blowing rate, the jets reduce the far-field noise at low frequencies, while their exact effect on high frequency noise is yet to be studied with the direct measurement of the far-field noise.

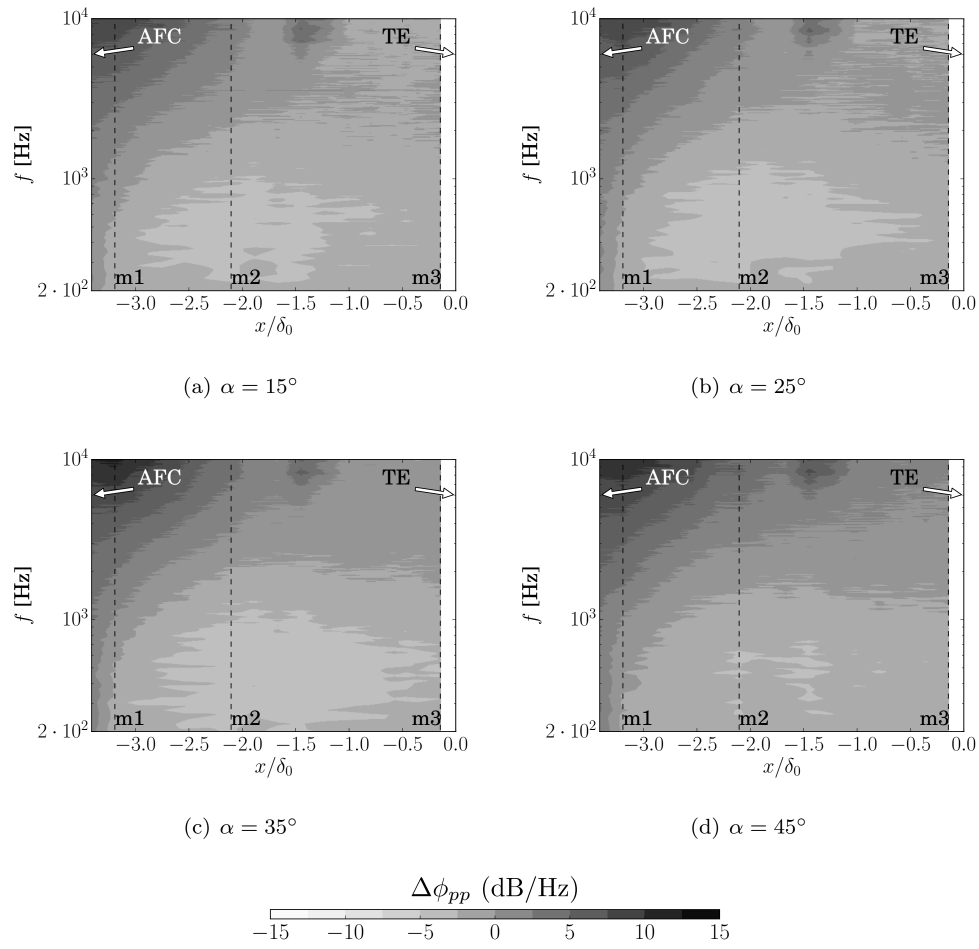

(a) $\alpha = 15°$

(b) $\alpha = 25°$

(c) $\alpha = 35°$

(d) $\alpha = 45°$

Figure 8. Changes in the surface pressure spectra for $\sigma = 0.4$ downstream of the active flow control section for $\alpha = 15 - 45°$ in $10°$ steps (dashed lines represent $m1$, $m2$ and $m3$)

The effect of the jet inclination was assessed by increasing α from 15° until 45° in steps of 10°. For each α, two blowing rates were applied, $\sigma = 0$ and $\sigma = 0.4$, each followed by measurements of the surface pressure fluctuations. From this, the changes in the power spectral density of the surface pressure fluctuations can be calculated as $\Delta\phi_{pp} = \phi_{pp,treated} - \phi_{pp,baseline}$ (dB/Hz), which are presented in Fig. 8. The dashed lines in Fig. 8 represent the locations of $m1$, $m2$ and $m3$. The results enable us to assess the effect of the jet inclination angle on the surface pressure fluctuations, and also to give an estimate of where the jets should be placed relative to the trailing edge exploit the effect of the jets at low frequencies on the trailing edge noise. Similarly to the results on $\overline{u}$ and u_{rms} (see Figs. 3, 4 and 5), it is observed that α has a negligible effect on the pressure spectra. The multiple jets injection increases the spectral content of the surface pressure fluctuations at high frequencies, while they are capable of attenuating it at low frequencies, which is consistent with the observations presented in Fig. 6. As α increases, the increase at high frequencies can be observed over longer streamwise distances. It can be seen that a streamwise distance exists, where the increase at high frequencies crosses the baseline level ($\Delta\phi_{pp} = 0$). After this particular location, the pressure fluctuations begin to increase in a broadband manner. From this, it can be concluded that the jet nozzles shall be located with respect to the trailing edge where the penalty in high frequencies cancels.

IV. Conclusions

The current work investigates a flow control technique for reduction of trailing edge noise. A spanwise array of inclined transverse jets was applied on a flat plate rig upstream of a sharp trailing edge. Three different angles of jet injection were considered, and the Reynolds number of the jets was also varied. The streamwise velocity component and the surface pressure fluctuations were measured at a number of locations downstream of the active flow control treatment. The turbulence statistics reveal that the interaction between the jets and the boundary layer generates a fluid layer characterised by a low energy content. According to Amiet's model of trailing edge noise, the product between the power spectra of surface pressure fluctuations (ϕ_{pp}) and the spanwise extent of turbulent length scales (Λ_z) is proportional to the far-field noise scattered from the trailing edge. The fluid layer associated with low energy content leads to the attenuation of ϕ_{pp} at low frequencies. The spanwise extent of turbulent length scales is also reduced by the application of the inclined jets. These effects suggest that the currently proposed method is capable of reducing the far-field noise generated by the interaction of turbulent boundary layer and trailing edge. The results show that the jet inclination has a negligible effect on the achieved reduction levels, while the aeroacoustic performance of the active flow control method is more sensitive to the applied jet velocity ratio. Future studies are needed to focus on the effects of jet spacing, jet diameter, and on the application of different velocity ratios. Measurements in anechoic conditions will also be carried out to effectively quantify the far-field noise production from the flat plate trailing edge, and to assess the performance of the micro-jet injection for the reduction of trailing edge noise.

References

[1]Brooks, T. F., Pope, D. S., and Marcolini, M. A., "Airfoil Self-Noise and Prediction," *NASA Report*, 1989.

[2]Williams, J. E. F. and Hawkings, D. L., "Sound Generation by Turbulence and Surfaces in Arbitrary Motion," *Philosophical Transactions of the Royal Society London*, 1969.

[3]Williams, J. E. F. and Hall, L. H., "Aerodynamic sound generation by turbulent flow and in the vicinity of a scattering half plane," *Journal of Fluid Mechanics*, 1970.

[4]Tam, C. K. W., "Discrete tones of isolated airfoils," *The Journal of the Acoustical Society of America*, Vol. 55, No. 6, 1974, pp. 1173–1177.

[5]Amiet, R. K., "Acoustic radiation from an airfoil in a turbulent stream," *Journal of Sound and Vibration*, Vol. 41, No. 4, 1975, pp. 407 – 420.

[6]Chase, D. M., "Noise radiated from an edge in turbulent flow," *AIAA Journal*, Vol. 13, No. 8, 1975, pp. 1041–1047.

[7]Amiet, R. K., "Noise Due to Turbulent Flow Past a Trailing Edge," *Journal of Sound and Vibration*, Vol. 47(3), 1976, pp. 387–393.

[8]Brooks, T. F. and Hodgson, T. H., "Trailing Edge Noise Prediction from Measured Surface Pressures," *Journal of Sound and Vibration*, 1981.

[9]Lyu, B., Azarpeyvand, M., and Sinayoko, S., "Prediction of noise from serrated trailing edges," *Journal of Fluid Mechanics*, Vol. 793, 2016, pp. 556–588.

[10]Gruber, M., *Airfoil noise reduction by edge treatments*, Ph.D. thesis, University of Southampton, 2012.

[11]Liu, X., Kamliya, H. J., Azarpeyvand, M., and Theunissen, R., "Wake Development of Airfoils with Serrated Trailing Edges," *22nd AIAA/CEAS Aeroacoustics Conference*, AIAA-2016-2817.

[12]Chong, T., Vathylakis, A., Joseph, P., and Gruber, M., "Self-Noise Produced by an Airfoil with Nonflat Plate Trailing-Edge Serrations," *AIAA Journal*, Vol. 51, No. 11, 2013, pp. 2665–2677.

[13]Chong, T. and Joseph, P., "An experimental study of airfoil instability tonal noise with trailing edge serrations," *Journal of Sound and Vibration*, Vol. 332, No. 24, 2013, pp. 6335–6358.

[14]Chong, T., Joseph, P., and Gruber, M., "Airfoil self noise reduction by non-flat plate type trailing edge serrations," *Applied Acoustics*, Vol. 74, No. 4, 2013, pp. 607–613.

[15]Gruber, M., Joseph, P., and Azarpeyvand, M., "An experimental investigation of novel trailing edge geometries on airfoil trailing edge noise reduction," *19th AIAA/CEAS Aeroacoustics Conference*, AIAA-2013-2011.

[16]Azarpeyvand, M., Gruber, M., and Joseph, P., "An analytical investigation of trailing edge noise reduction using novel serrations," *19th AIAA/CEAS Aeroacoustics Conference*, AIAA-2013-2009.

[17]Finez, A., Jondeau, E., Roger, M., and Jacob, M., "Broadband noise reduction with trailing edge brushes," *16th AIAA/CEAS Aeroacoustics Conference*, AIAA-2010-3980.

[18]Herr, M. and Dobrzynski, W., "Experimental Investigations in Low-Noise Trailing-Edge Design," *AIAA Journal*, Vol. 43, No. 6, June 2005.

[19]Geyer, T., Sarradj, E., and Fritzsche, C., "Porous airfoils: noise reduction and boundary layer effects," *15th AIAA/CEAS Aeroacoustics Conference*, No. May, 2009, pp. 1–18.

[20]Geyer, T., Sarradj, E., and Fritzsche, C., "Measurement of the noise generation at the trailing edge of porous airfoils," *Experiments in Fluids*, Vol. 48, No. 2, 2010, pp. 291–308.

[21]Howe, M., "On the Added Mass of a Perforated Shell, with Application to the Generation of Aerodynamic Sound by a Perforated Trailing Edge," *Proceedings of the Royal Society of London. Series A, Mathematical and Physical Sciences*, Vol. 365, No. 1721, 1979, pp. 209–233.

[22]Showkat Ali, S., Liu, X., and Azarpeyvand, M., "Bluff Body Flow and Noise Control Using Porous Media," *22nd AIAA/CEAS Aeroacoustics Conference*, AIAA-2016-2754.

[23]Showkat Ali, S., Szőke, M., and Azarpeyvand, M., "Trailing Edge Bluntness Flow and Noise Control Using Porous Treatments," *22nd AIAA/CEAS Aeroacoustics Conference*, AIAA-2016-2832.

[24]Liu, H., Azarpeyvand, M., Weia, J., and Qua, Z., "Tandem cylinder aerodynamic sound control using porous coating," *Journal of Sound and Vibration*, , No. 334, 2014, pp. 190–201.

[25]Afshari, A., Azarpeyvand, M., Dehghan, A. A., and Szőke, M., "Trailing Edge Noise Reduction Using Novel Surface Treatments," *22nd AIAA/CEAS Aeroacoustics Conference*, AIAA-2016-2834.

[26]Afshari, A., Azarpeyvand, M., Dehghan, A. A., and Szőke, M., "Three-Dimensional Surface Treatments for Trailing Edge Noise Reduction," *23rd International Congress on Sound & Vibration, Athens, Greece*, 2016.

[27]Clark, I., Baker, D., Alexander, W. N., Devenport, W., Glegg, S. A., Jaworski, J., and Peake, N., "Experimental and Theoretical Analysis of Bio-Inspired Trailing Edge Noise Control Devices," *22nd AIAA/CEAS Aeroacoustics Conference*, 2016, p. 3020.

[28]Clark, I., Alexander, W. N., Devenport, W., Glegg, S. A., Jaworski, J., Daily, C., and Peake, N., "Bio-Inspired Trailing Edge Noise Control," *21nd AIAA/CEAS Aeroacoustics Conference*, 2015, p. 2365.

[29]Ai, Q., Azarpeyvand, M., Lachenal, X., and Weaver, P. M., "Aerodynamic and aeroacoustic performance of airfoils with morphing structures," *Wind Energy*, Vol. 19, No. 7, 2016, pp. 1325–1339, we.1900.

[30]R. R. Parchen and Technisch Physisce Dienst, "Progress report DRAW: A prediction scheme for trailing edge noise based on detailed boundary layer characteristics," *TNO Report*, Vol. HAG-RPT-980023, 1998.

[31]Bertagnolio, F., "Trailing Edge Noise Model Applied to Wind Turbine Airfoils," *Riso Report*, 2008.

[32]Szőke, M. and Azarpeyvand, M., "Active Flow Control Methods for the Reduction of Trailing Edge Noise," *23rd AIAA/CEAS Aeroacoustics Conference*, AIAA-2017-3004.

[33]Muppidi, S. and Mahesh, K., "Direct numerical simulation of round turbulent jets in crossflow," *Journal of Fluid Mechanics*, Vol. 574, 2007, pp. 59.

[34]Fric, T. F. and Roshko, A., "Vortical structure in the wake of a transverse jet," *Journal of Fluid Mechanics*, Vol. 279, No. 1994, 1994, pp. 1–47.

[35]Mahesh, K., "The Interaction of Jets with Crossflow," *Annual Review of Fluid Mechanics*, Vol. 45, No. 1, 2013, pp. 379–407.

[36]Pietrzyk, J., Bogard, D., and Crawford, M., "Hydrodynamic measurements of jets in crossflow for gas turbine film cooling applications," *ASME J. Turbomach*, Vol. 111, No. 2, 1989, pp. 139–145.

[37]Hyams, D. G. and Leylek, J. H., "A detailed analysis of film cooling physics: part IIIstreamwise injection with shaped holes," *International Gas Turbine and Aeroengine Congress and Exhibition*, ASME, 1997.

[38]Walters, D. K. and Leylek, J. H., "A detailed analysis of film–cooling physics: Part istreamwise injection with cylindrical holes," *International Gas Turbine and Aeroengine Congress and Exhibition*, ASME, 1997.

[39]Burd, S. W., Kaszeta, R. W., and Simon, T. W., "Measurements in film cooling flows: hole L/D and turbulence intensity effects," *Journal of Turbomachinery*, Vol. 120, No. 4, 1998, pp. 791–798.

[40]Bogard, D. and Thole, K., "Gas turbine film cooling," *Journal of Propulsion and Power*, Vol. 22, No. 2, 2006, pp. 249–270.

[41]Iourokina, I. V. and Lele, S. K., "Large eddy simulation of film cooling flow above a flat plate from inclined cylindrical holes," *ASME 2nd Joint US European Fluid Engineering Summer Meeting, Miami, FL, July*, 2006, pp. 17–20.

[42]Rozati, A. and Tafti, D. K., "Large-eddy simulations of leading edge film cooling: Analysis of flow structures, effectiveness, and heat transfer coefficient," *International Journal of Heat and Fluid Flow*, Vol. 29, No. 1, 2008, pp. 1–17.

[43]Kline, S. J. and McClintock, F. A., "Describing uncertainties in single-sample experiments," *Mechanical Engineering*, Vol. 75, No. 1, Jan 1953, pp. 3–8.

[44]Schewe, G., "On the structure and resolution of wall-pressure fluctuations associated with turbulent boundary-layer flow," *Journal of Fluid Mechanics*, Vol. 134, 1983, pp. 311–328.

[45]Corcos, G. M., "Resolution of Pressure in Turbulence," *The Journal of the Acoustical Society of America*, Vol. 35, No. 2, 1963, pp. 192–199.

[46]Gray, R. M. and Goodman, J. W., *Fourier Transforms: An Introduction for Engineers*, Vol. 322, Springer Science & Business Media, 2012.

[47]Antonia, R. A., Zhu, Y., and Sokolov, M., "Effect of concentrated wall suction on a turbulent boundary layer," *Physics of Fluids*, Vol. 7, No. 10, 1995, pp. 2465–2474.